Erratum 15 February 2017. See Erratum.

design of a self-sustained, completely synthetic carbon metabolism in artificial or minimal cells (*37*).

REFERENCES AND NOTES

1. I. A. Berg, *Appl. Environ. Microbiol.* **77**, 1925–1936 (2011).
2. G. Fuchs, *Annu. Rev. Microbiol.* **65**, 631–658 (2011).
3. M. Aresta, in *Greenhouse Gases: Mitigation and Utilization, CHEMRAWN-XVII and ICCDU-IX Conference, July 8 to 12, 2007*, E. Buncel, Ed. (Queen's University, Kingston, Ontario, Canada, 2009), pp. 123–149.
4. S. M. Glueck, S. Gümüs, W. M. F. Fabian, K. Faber, *Chem. Soc. Rev.* **39**, 313–328 (2010).
5. L. Rosgaard, A. J. de Porcellinis, J. H. Jacobsen, N. U. Frigaard, Y. Sakuragi, *J. Biotechnol.* **162**, 134–147 (2012).
6. B. J. Walker, A. VanLoocke, C. J. Bernacchi, D. R. Ort, *Annu. Rev. Plant Biol.* **67**, 107–129 (2016).
7. T. J. Erb, J. Zarzycki, *Curr. Opin. Chem. Biol.* **34**, 72–79 (2016).
8. D. N. Greene, S. M. Whitney, I. Matsumura, *Biochem. J.* **404**, 517–524 (2007).
9. N. E. Kreel, F. R. Tabita, *PLOS ONE* **10**, e0138351 (2015).
10. P. M. Shih, J. Zarzycki, K. K. Niyogi, C. A. Kerfeld, *J. Biol. Chem.* **289**, 9493–9500 (2014).
11. R. Kebeish *et al.*, *Nat. Biotechnol.* **25**, 593–599 (2007).
12. M. Mattozzi, M. Ziesack, M. J. Voges, P. A. Silver, J. C. Way, *Metab. Eng.* **16**, 130–139 (2013).
13. M. W. Keller *et al.*, *Proc. Natl. Acad. Sci. U.S.A.* **110**, 5840–5845 (2013).
14. N. Antonovsky *et al.*, *Cell* **166**, 115–125 (2016).
15. A. Bar-Even, E. Noor, N. E. Lewis, R. Milo, *Proc. Natl. Acad. Sci. U.S.A.* **107**, 8889–8894 (2010).
16. P. H. Opgenorth, T. P. Korman, J. U. Bowie, *Nat. Chem. Biol.* **12**, 393–395 (2016).
17. S. Billerbeck, M. Bujara, C. Hold, R. Pellaux, S. Panke, *FEBS J.* **277** (suppl. 1), 23 (2010).
18. C. E. Hodgman, M. C. Jewett, *Metab. Eng.* **14**, 261–269 (2012).
19. J. A. Rollin, T. K. Tam, Y. H. P. Zhang, *Green Chem.* **15**, 1708–1719 (2013).
20. S. P. Long, E. A. Ainsworth, A. Rogers, D. R. Ort, *Annu. Rev. Plant Biol.* **55**, 591–628 (2004).
21. R. J. Spreitzer, M. E. Salvucci, *Annu. Rev. Plant Biol.* **53**, 449–475 (2002).
22. M. Könneke *et al.*, *Proc. Natl. Acad. Sci. U.S.A.* **111**, 8239–8244 (2014).
23. L. Schada von Borzyskowski, R. G. Rosenthal, T. J. Erb, *J. Biotechnol.* **168**, 243–251 (2013).
24. T. J. Erb *et al.*, *Proc. Natl. Acad. Sci. U.S.A.* **104**, 10631–10636 (2007).
25. D. M. Peter *et al.*, *Angew. Chem. Int. Ed.* **54**, 13457–13461 (2015).
26. T. J. Erb, V. Brecht, G. Fuchs, M. Müller, B. E. Alber, *Proc. Natl. Acad. Sci. U.S.A.* **106**, 8871–8876 (2009).
27. M. Volpers *et al.*, *PLOS ONE* **11**, e0157851 (2016).
28. T. J. Erb, G. Fuchs, B. E. Alber, *Mol. Microbiol.* **73**, 992–1008 (2009).
29. B. W. Carlson, L. L. Miller, *J. Am. Chem. Soc.* **105**, 7453–7454 (1983).
30. V. de Lorenzo, A. Sekowska, A. Danchin, *FEMS Microbiol. Rev.* **39**, 96–119 (2015).
31. C. Lerma-Ortiz *et al.*, *Biochem. Soc. Trans.* **44**, 961–971 (2016).
32. C. L. Linster *et al.*, *J. Biol. Chem.* **286**, 42992–43003 (2011).
33. N. L. Gale, J. V. Beck, *J. Bacteriol.* **94**, 1052–1059 (1967).
34. F. Jacob, *Science* **196**, 1161–1166 (1977).
35. D. R. Ort *et al.*, *Proc. Natl. Acad. Sci. U.S.A.* **112**, 8529–8536 (2015).
36. R. K. Yadav *et al.*, *J. Am. Chem. Soc.* **134**, 11455–11461 (2012).
37. C. A. Hutchison III *et al.*, *Science* **351**, aad6253 (2016).
38. P. C. Hinkle, *BBA Bioenergetics* **1706**, 1–11 (2005).
39. D. M. Kramer, J. R. Evans, *Plant Physiol.* **155**, 70–78 (2011).
40. L. Schada von Borzyskowski, M. Remus-Emsermann, R. Weishaupt, J. A. Vorholt, T. J. Erb, *ACS Synth. Biol.* **4**, 430–443 (2015).

ACKNOWLEDGMENTS

We thank G. Fuchs for introducing us to the fundamental principles of microbial CO_2 fixation. We thank U. Oppermann for the expression plasmid p2BP1, K. Castiglione for the expression plasmid of Fdh (D221A), J. Andexer for the expression plasmid for Pkk2 and the purified enzyme, and J. Zarzycki and B. Vögeli for contributions during pathway design. The work conducted by the U.S. Department of Energy Joint Genome Institute, a DOE Office of Science User Facility, is supported under contract DE-AC02-05CH11231. Also supported by European Research Council grant ERC 637675 "SYBORG," Swiss National Science Foundation Ambizione grant PZ00P3_136828/1, ETH Zürich grant ETH-41 12-2, and the Max Planck Society. Supporting data are available in the supplementary materials. Author contributions: T.J.E. conceived the project; T.J.E., L.S.v.B., and T.S. designed the experiments, analyzed the data, and wrote the manuscript; T.J.E., T.S., and L.S.v.B. performed experiments; S.B. assisted in experiments; and N.S.C. performed mass spectrometry and analyzed the data.

SUPPLEMENTARY MATERIALS

www.sciencemag.org/content/354/6314/900/suppl/DC1
Materials and Methods
Supplementary Text
Figs. S1 to S14
Tables S1 to S8
References (*41*–*63*)

8 July 2016; accepted 5 October 2016
10.1126/science.aah5237

NEURODEGENERATION

Site-specific phosphorylation of tau inhibits amyloid-β toxicity in Alzheimer's mice

Arne Ittner,[1]* Sook Wern Chua,[1] Josefine Bertz,[1] Alexander Volkerling,[1] Julia van der Hoven,[1] Amadeus Gladbach,[1] Magdalena Przybyla,[1] Mian Bi,[1] Annika van Hummel,[1,2] Claire H. Stevens,[1] Stefania Ippati,[1] Lisa S. Suh,[1,3] Alexander Macmillan,[4] Greg Sutherland,[3] Jillian J. Kril,[3] Ana P. G. Silva,[5] Joel P. Mackay,[5] Anne Poljak,[6] Fabien Delerue,[1,7] Yazi D. Ke,[2] Lars M. Ittner[1,7,8]*

Amyloid-β (Aβ) toxicity in Alzheimer's disease (AD) is considered to be mediated by phosphorylated tau protein. In contrast, we found that, at least in early disease, site-specific phosphorylation of tau inhibited Aβ toxicity. This specific tau phosphorylation was mediated by the neuronal p38 mitogen-activated protein kinase p38γ and interfered with postsynaptic excitotoxic signaling complexes engaged by Aβ. Accordingly, depletion of p38γ exacerbated neuronal circuit aberrations, cognitive deficits, and premature lethality in a mouse model of AD, whereas increasing the activity of p38γ abolished these deficits. Furthermore, mimicking site-specific tau phosphorylation alleviated Aβ-induced neuronal death and offered protection from excitotoxicity. Our work provides insights into postsynaptic processes in AD pathogenesis and challenges a purely pathogenic role of tau phosphorylation in neuronal toxicity.

Alzheimer's disease (AD), the most prevalent form of dementia, is neuropathologically characterized by extracellular amyloid-β (Aβ) plaques and intracellular tau-containing neurofibrillary tangles (*1*, *2*). Growing evidence suggests that Aβ and tau together orchestrate neuronal dysfunction in AD (*3*), although their molecular connections remain poorly understood. Aberrant tau phosphorylation is the first step in a cascade leading to its deposition and to cognitive dysfunction (*4*, *5*). Aβ is thought to trigger toxic events, including tau phosphorylation (*6*). Accordingly, the depletion of tau prevents Aβ toxicity in AD models (*7*–*9*). Aβ-induced neuronal network and synaptic dysfunction is associated with aberrant glutamatergic synaptic transmission (*10*). *N*-methyl-D-aspartate (NMDA)–type glutamatergic receptors (NRs) drive glutamate-induced neuronal excitotoxicity (*11*) and mediate Aβ toxicity by downstream responses that promote neuronal dysfunction (*12*).

Multiple factors, including p38 kinases, contribute to NR-mediated toxicity (*12*). Although inhibition of p38α and p38β improves Aβ-induced long-term potentiation deficits (*13*, *14*), it increases hyperexcitability in Aβ precursor protein (APP) transgenic mice (*15*). However, the specificity of p38 inhibitors remains debatable (*16*, *17*). Other p38 kinases, p38γ and p38δ, have not been studied in AD. To understand the roles of p38 kinases in AD, we induced excitotoxic seizures with pentylenetetrazole (PTZ), an approach widely used for studying excitotoxicity in AD mouse models (*8*, *9*). We used mice with individual deletion of *p38α*, *p38β*, *p38γ*, or *p38δ* (fig. S1). Surprisingly, only *p38γ* depletion ($p38\gamma^{-/-}$), but not systemic *p38β*, *p38δ*, or neuronal *p38α* ($p38\alpha^{\Delta neu}$)

[1]Dementia Research Unit, School of Medical Sciences, University of New South Wales (UNSW), Sydney, New South Wales 2052, Australia. [2]Motor Neuron Disease Unit, School of Medical Sciences, UNSW, Sydney, New South Wales 2052, Australia. [3]Discipline of Pathology, Sydney Medical School, University of Sydney, Sydney, New South Wales 2050, Australia. [4]Biomedical Imaging Facility, Mark Wainwright Analytical Centre, UNSW, Sydney, New South Wales 2052, Australia. [5]School of Molecular Bioscience, University of Sydney, Sydney, New South Wales 2050, Australia. [6]Biomedical Mass Spectrometry Facility, Mark Wainwright Analytical Centre, UNSW, Sydney, New South Wales 2052, Australia. [7]Transgenic Animal Unit, Mark Wainwright Analytical Centre, UNSW, Sydney, New South Wales 2052, Australia. [8]Neuroscience Research Australia, Sydney, New South Wales 2031, Australia.
***Corresponding author. Email: a.ittner@unsw.edu.au (A.I.); l.ittner@unsw.edu.au (L.M.I.)**

Downloaded from http://science.sciencemag.org/ on July 18, 2017

Erratum 15 February 2017. See full text.

knockout, changed PTZ-induced seizures (Fig. 1A and fig. S2). Pan-p38 inhibition in wild-type (WT) mice augmented seizures, similar to the effects of *p38*γ depletion (fig. S3). Consistent with a postsynaptic role, only p38γ localized to dendritic spines and postsynaptic densities (PSDs) of neurons and was enriched in PSD preparations (Fig. 1B and fig. S4). Hence, of all p38 kinases, only p38γ localized to postsynapses and limited excitotoxicity.

To test whether $p38\gamma^{-/-}$ augments Aβ-induced deficits, we crossed $p38\gamma^{-/-}$ with Aβ-forming APP23 mice. APP23 mice present with premature mortality, memory deficits, neuronal circuit aberrations with epileptiform brain activity,

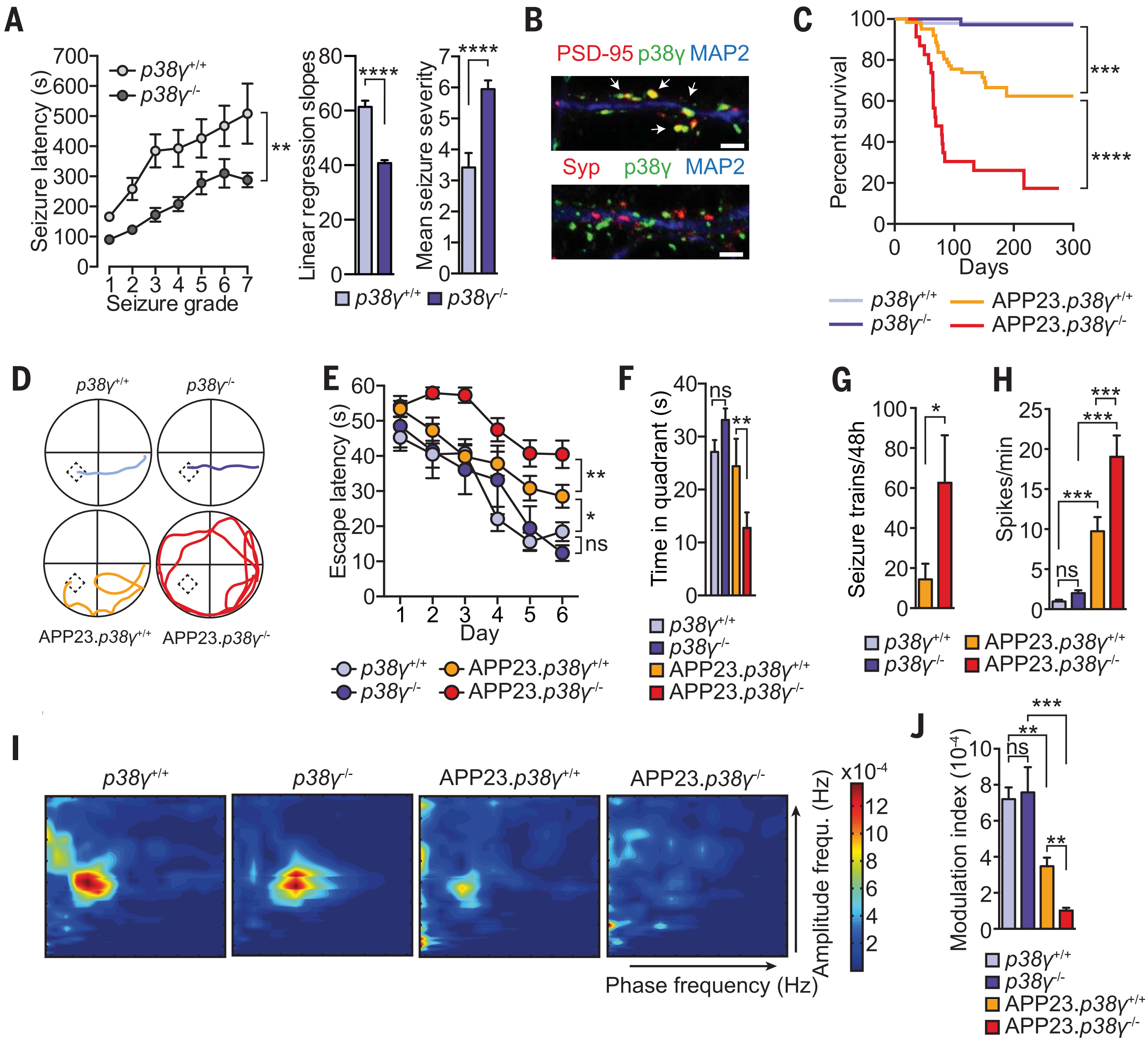

Fig. 1. Depletion of postsynaptic p38γ exacerbates excitotoxicity and deficits in APP transgenic mice. (**A**) Reduced seizure latency (linear regression slopes) and increased seizure severity in $p38\gamma^{-/-}$ mice compared with $p38\gamma^{+/+}$ animals injected with 30 mg/kg pentylenetetrazole (PTZ) (n = 10 to 12 mice). (**B**) Colocalization of p38γ and postsynaptic PSD-95 (arrows), but not presynaptic synaptophysin (Syp), in neurons. Scale bars, 1 μm. (**C**) Mortality in APP23.$p38\gamma^{+/+}$ mice was further augmented in APP23.$p38\gamma^{-/-}$ animals, whereas $p38\gamma^{+/+}$ and $p38\gamma^{-/-}$ mice survived normally (n = 43 to 62). (**D** to **F**) Memory deficits in 4-month-old APP23.$p38\gamma^{+/+}$ and APP23.$p38\gamma^{-/-}$ mice (memory deficits were exacerbated in the APP23.$p38\gamma^{-/-}$ animals). Morris water maze (MWM) test: (D) Representative MWM path traces to a hidden platform. (E) Increased escape latency and (F) reduced time in the target quadrant during probe trials in APP23.$p38\gamma^{+/+}$ and, more so, APP23.$p38\gamma^{-/-}$ mice compared with $p38\gamma^{+/+}$ and $p38\gamma^{-/-}$ mice (n = 8 to 10). (**G** to **H**) Increased (G) spike train and (H) spike frequency in APP23.$p38\gamma^{+/+}$ and APP23.$p38\gamma^{-/-}$ mice but not $p38\gamma^{+/+}$ and $p38\gamma^{-/-}$ mice (n = 6 to 8). (**I**) Representative phase-amplitude comodulograms of interictal hippocampal local field potential recordings showed reduced and virtually lost cross-frequency coupling (CFC) (~8 Hz) in APP23.$p38\gamma^{+/+}$ and APP23.$p38\gamma^{-/-}$ mice, respectively, compared with $p38\gamma^{+/+}$ and $p38\gamma^{-/-}$ mice. (**J**) Reduced modulation index in APP23.$p38\gamma^{+/+}$ mice and, more so, in APP23.$p38\gamma^{-/-}$ mice compared with $p38\gamma^{+/+}$ and $p38\gamma^{-/-}$ animals (n = 6 to 8). For (A), (C), (E) to (H), and (J): ****$P < 0.0001$, ***$P < 0.001$, **$P < 0.01$, *$P < 0.05$; ns, not significant. Error bars indicate SEM.

Downloaded from http://science.sciencemag.org/ on July 18, 2017

Erratum 15 February 2017. See full text.

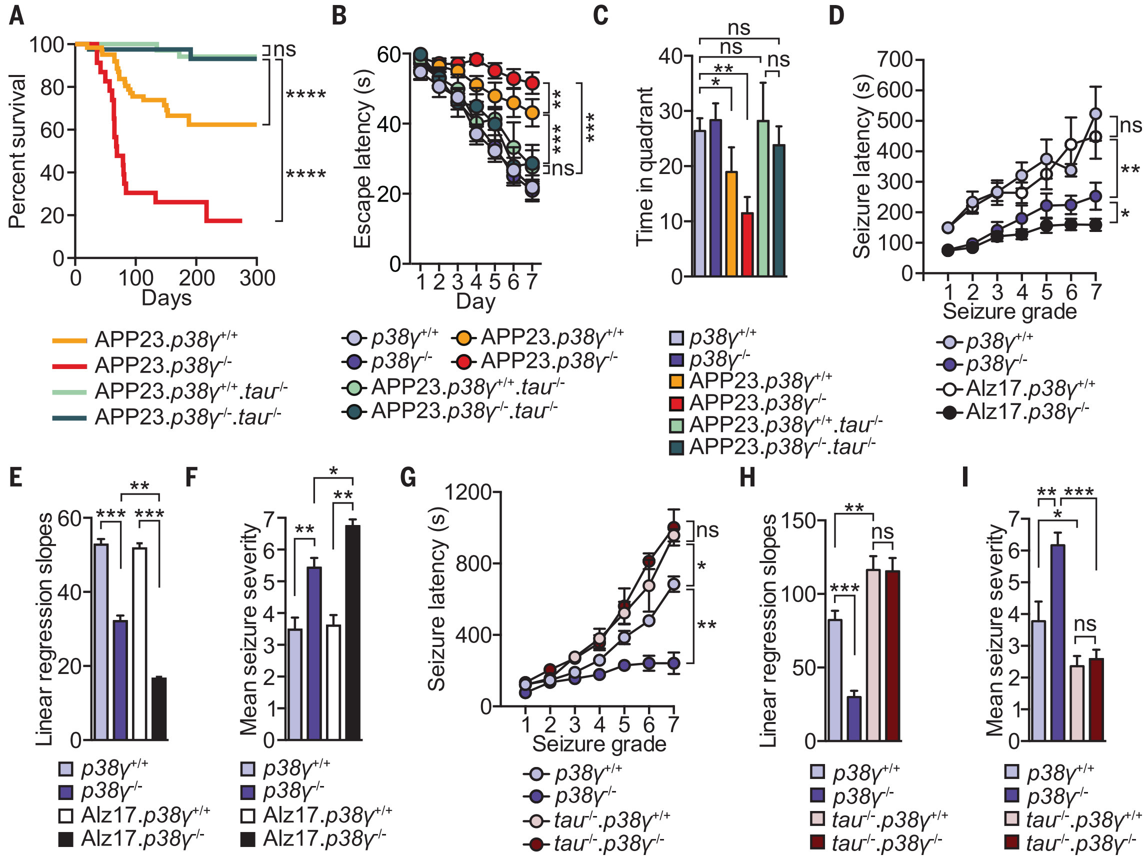

Fig. 2. Tau is required for p38γ-mediated inhibition of Aβ and excitotoxicity. (**A**) Normal survival of APP23.$p38\gamma^{-/-}$.$tau^{-/-}$ compared with APP23.$p38\gamma^{-/-}$ and APP23.$p38\gamma^{+/+}$ mice (n = 42 to 62). (**B** and **C**) Normal memory in 12-month-old APP23.$p38\gamma^{-/-}$.$tau^{-/-}$ mice compared with APP23.$p38\gamma^{-/-}$ and APP23.$p38\gamma^{+/+}$ mice (n = 10 to 12). MWM test: (B) Escape latency and (C) time in target quadrant during probe trials. (**D** to **F**) (D) Further reduction in seizure latencies, shown by linear regression analysis (E). (F) Further enhanced mean seizure severity following 30 mg/kg PTZ in Alz17.$p38\gamma^{-/-}$ mice versus those already reduced in $p38\gamma^{-/-}$ compared with $p38\gamma^{+/+}$ and Alz17.$p38\gamma^{+/+}$ mice (n = 10 to 12). (**G** to **I**) (G) Seizure latencies after 30 mg/kg PTZ were reduced, as shown by linear regression analysis (H), and mean seizure severity was increased in $tau^{+/+}$.$p38\gamma^{-/-}$ compared with $tau^{+/+}$.$p38\gamma^{+/+}$ mice (I). However, latencies were markedly increased (G) and severities similarly reduced (I) in both $tau^{-/-}$.$p38\gamma^{+/+}$ and $tau^{-/-}$.$p38\gamma^{-/-}$ mice (n = 10 to 12). For all panels: ****$P < 0.0001$, ***$P < 0.001$, **$P < 0.01$, *$P < 0.05$; ns, not significant. Error bars indicate SEM.

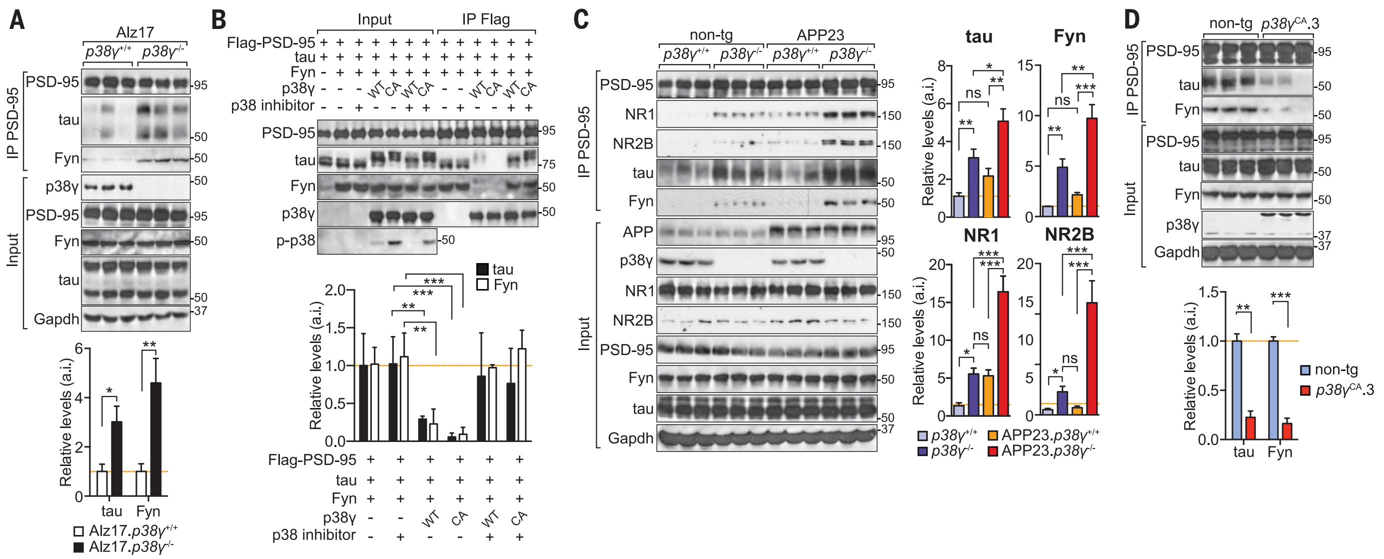

Fig. 3. Active p38γ dissociates PSD-95/tau/Fyn/NR complexes. (**A**) Immunoprecipitation (IP) analysis. More PSD-95/tau/Fyn complexes were immunoprecipitated from the brains of Alz17.$p38\gamma^{-/-}$ than Alz17.$p38\gamma^{+/+}$ animals, despite comparable total protein levels. Detection of glyceraldehyde-3-phosphate dehydrogenase (GAPDH) confirmed equal loading (n = 6). Numbers at right indicate molecular weight. a.i., arbitrary index. (**B**) p38γ (WT) and $p38\gamma^{CA}$ (CA) failed to disrupt PSD-95/tau/Fyn complexes in the presence of the p38 inhibitor (n = 6). p38 inhibition reduces phosphorylated active p38 levels (p-p38). (**C**) More tau, Fyn, and NMDA receptor subunits 1 (NR1) and 2B (NR2B) were immunoprecipitated with PSD-95 from $p38\gamma^{-/-}$ versus $p38\gamma^{+/+}$ brains. This result was further enhanced in APP23.$p38\gamma^{-/-}$ mice compared with APP23.$p38\gamma^{+/+}$ animals, without changes to total protein levels (n = 6 to 8). (**D**) Virtually no PSD-95/tau/Fyn complexes were immunoprecipitated from the brains of $p38\gamma^{CA}$-expressing mice (n = 6). For all panels: Representative blots are shown. Quantification of IP bands relative to PSD-95 IP. ***$P < 0.001$; **$P < 0.01$; *$P < 0.05$. Error bars indicate SEM.

Downloaded from http://science.sciencemag.org/ on July 18, 2017

Erratum 15 February 2017. See full text.

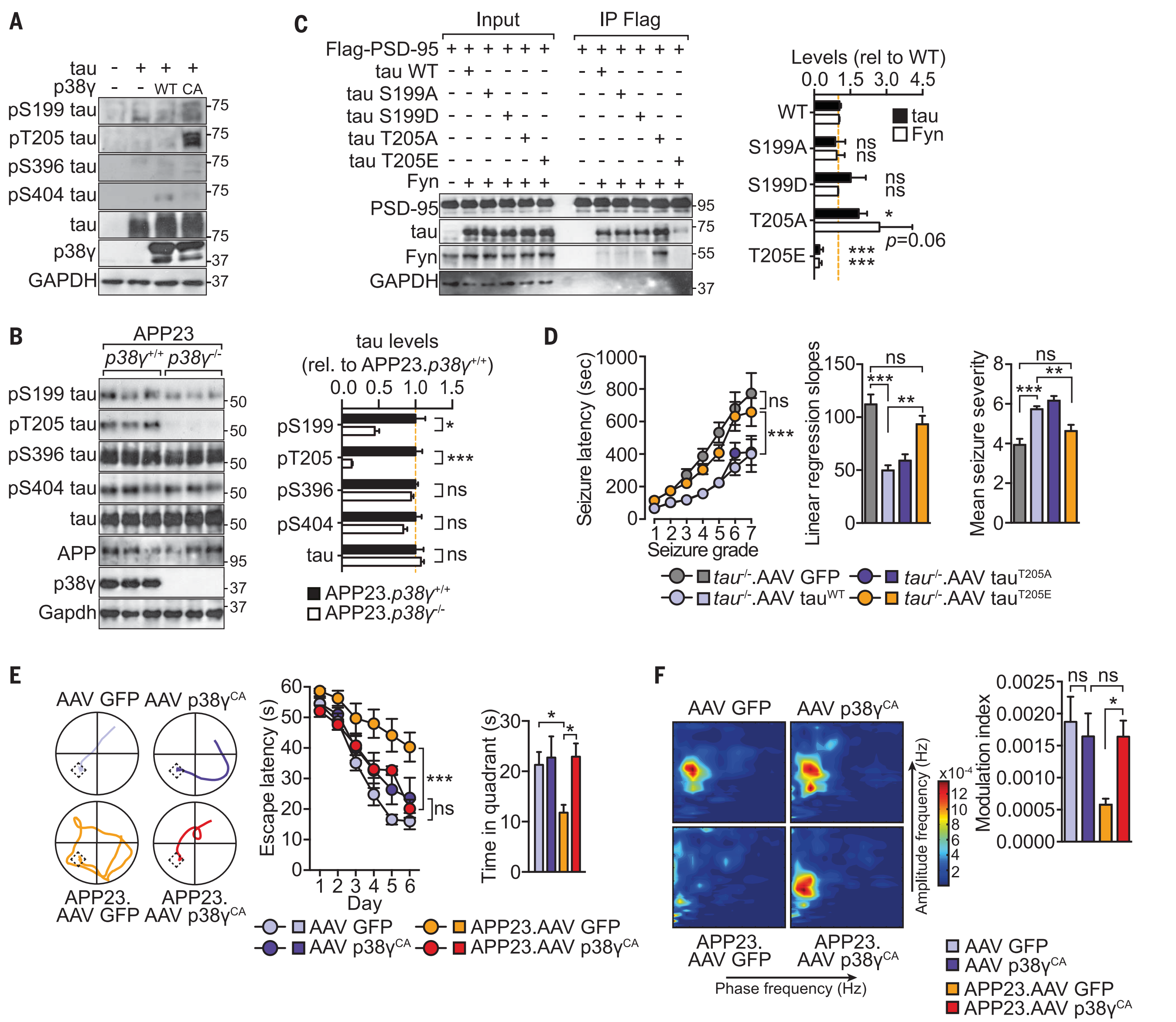

Fig. 4. Site-specific tau phosphorylation disrupts PSD-95/tau/Fyn interaction and inhibits Aβ toxicity. (**A**) Coexpression of p38γ (WT) or p38γ^{CA} (CA) with tau showed phosphorylation at T205, less at S199, and virtually none at S396 or S404. Detection of GAPDH confirmed equal loading. (**B**) Compared with APP23.*p38*γ$^{+/+}$ animals, APP23.*p38*γ$^{-/-}$ mice showed a lack of T205 tau phosphorylation (n = 6). Other sites remained phosphorylated. Graph shows quantification of tau phosphorylation. (**C**) Coexpression of T205E disrupted PSD95/tau/Fyn IP, whereas T205A tau increased it (n = 6). S199 mutations had no effect. Graph shows quantification of tau/Fyn bound to PSD-95. D, Asp. (**D**) AAV-mediated expression of WT and T205A, but not T205E or GFP, restored susceptibility of *tau*$^{-/-}$ to 50 mg/kg PTZ-induced seizures, with reduced latency (linear regression) and higher severity (n = 12). (**E**) Improved memory in APP23 mice upon AAV-mediated p38γ^{CA} expression (APP23.AAV^{p38γCA}). MWM test: (Left) Example traces; (middle) escape latencies; (right) time in target quadrant during probe trials (n = 8 to 10). (**F**) Rescued CFC in APP23.AAV^{p38γCA} compared with APP23.AAV^{GFP} mice (n = 5 to 6). For (B) to (F): ***P < 0.001; **P < 0.01; *P < 0.05; ns, not significant. Error bars indicate SEM.

and Aβ pathology (*9*, *15*, *18*). Compared with APP23.*p38*γ$^{+/+}$ mice, APP23.*p38*γ$^{-/-}$ animals had increased sensitivity to PTZ-induced seizures (fig. S5). Aβ pathology was comparable in the brains of APP23.*p38*γ$^{-/-}$ and APP23.*p38*γ$^{+/+}$ mice (fig. S6), but *p38*γ deletion aggravated premature mortality and memory deficits of APP23 mice (Fig. 1, C to F, and fig. S7). *p38*γ$^{-/-}$ mice showed no deficits and had normal motor function (fig. S8). Electroencephalography showed enhanced spontaneous epileptiform activity and interictal hypersynchronous discharges in APP23.*p38*γ$^{-/-}$ compared with APP23.*p38*γ$^{+/+}$ mice (Fig. 1, G and H, and fig. S9). Hippocampal theta and gamma oscillations and cross-frequency coupling (CFC) through theta-phase modulation of gamma power are measures of network activity related to memory, including in humans (*19*–*22*). These measures are compromised in APP transgenic mice (*15*). Compromised spectral power and CFC of APP23.*p38*γ$^{+/+}$ mice were significantly more affected in APP23.*p38*γ$^{-/-}$ recordings (Fig. 1, I and J, and fig. S9). Recordings of *p38*γ$^{-/-}$ and *p38*γ$^{+/+}$ mice were indistinguishable. In summary, p38γ depletion exacerbated excitotoxicity, neuronal circuit synchronicity, mortality, and memory deficits in APP23 mice, without changes in Aβ pathology. In addition, p38γ levels were reduced in aged APP23 and APP$^{NL\text{-}G\text{-}F}$ mice and humans with AD (fig. S10), further suggesting that the loss of p38γ-mediated neuroprotection may contribute to AD pathogenesis.

To determine whether the Aβ toxicity–limiting effects of p38γ were tau-dependent, we crossed

Downloaded from http://science.sciencemag.org/ on July 18, 2017

Erratum 15 February 2017. See full text.

APP23.*p38*γ$^{-/-}$ with *tau*$^{-/-}$ mice. The exacerbating effects of p38γ loss on reduced survival, memory deficits, and neuronal network dysfunction of APP23 mice were virtually abolished in APP23.*p38*γ$^{-/-}$.*tau*$^{-/-}$ mice (Fig. 2, A to C, and fig. S11). These data also showed that, compared with APP23 mice, APP23.*p38*γ$^{-/-}$ animals had aggravated memory deficits that persisted with aging. In contrast, increasing tau levels in *p38*γ$^{-/-}$ mice [brought about by crossing with nonmutant tau-expressing Alz17 mice (*23*)] significantly enhanced PTZ-induced seizures in Alz17.*p38*γ$^{-/-}$ mice (Fig. 2, D to F). Conversely, when compared to *tau*$^{-/-}$.*p38*γ$^{+/+}$ mice, *tau*$^{-/-}$.*p38*γ$^{-/-}$ animals showed similar protection from PTZ-induced seizures (Fig. 2, G to I). Taken together, the effects of p38γ on excitotoxicity and Aβ toxicity were tau-dependent.

We have previously shown that postsynaptic PSD-95/tau/Fyn complexes mediate Aβ-induced excitotoxicity (*9*). PSD-95/tau/Fyn interaction was enhanced in Alz17.*p38*γ$^{-/-}$ animals versus Alz17.*p38*γ$^{+/+}$ mice (Fig. 3A and fig. S12). Conversely, no PSD-95/tau/Fyn complexes were isolated from *tau*$^{-/-}$ and *tau*$^{-/-}$.*p38*γ$^{-/-}$ brains (fig. S12). Increasing p38γ levels compromised PSD-95/tau/Fyn interaction in cells, and expression of a constitutively active p38γ variant (p38γ^{CA}) completely abolished this interaction (Fig. 3B and fig. S13). Pan-p38 inhibition stopped p38γ/p38γ^{CA}-induced disruption of PSD-95/tau/Fyn complexes (Fig. 3B). PSD-95 copurified more tau and Fyn from *p38*γ$^{-/-}$ versus *p38*γ$^{+/+}$ brains, and even more from APP23.*p38*γ$^{-/-}$ compared with APP23.*p38*γ$^{+/+}$ and *p38*γ$^{-/-}$ brains (Fig. 3C). Conversely, PSD-95/tau/Fyn interaction was reduced in transgenic mice with neuronal expression of p38γ^{CA} (Fig. 3D and fig. S14). PTZ transiently increased PSD-95/tau/Fyn complex formation in *p38*γ$^{+/+}$ animals; this effect was even more noticeable in *p38*γ$^{-/-}$ mice (fig. S12). Fyn-mediated NR2B phosphorylation at Tyr[1472] (Y1472) facilitates PSD-95/NR2B interaction (*24*). Consistent with increased PSD-95/tau/Fyn complex formation, NR2B phosphorylation at Y1472 was increased in *p38*γ$^{-/-}$ brains (fig. S15). Conversely, cellular expression of p38γ and p38γ^{CA}—but not p38α^{CA}, p38β^{CA}, or p38δ^{CA}—reduced Y1472 phosphorylation of NR2B (fig. S15). Hence, p38γ regulated PSD-95/tau/Fyn complexes, likely at the level of PSD-95/tau interaction (fig. S16).

Although p38γ hyperphosphorylates tau during long-term in vitro kinase assays (*25*), the temporal profile of p38γ-induced tau phosphorylation in acute signaling remains unknown. Short-term in vitro kinase reactions using phosphorylation site–specific tau antibodies revealed phosphorylation at Ser[199] (S199), Thr[205] (T205), S396, and S404 (fig. S17). Mass spectrometric analysis confirmed these and 14 additional, though low-abundant, sites (figs. S17C and S18 and table S4). Coexpression of p38γ or p38γ^{CA} and tau in cells revealed tau phosphorylation (p) at T205, less at S199, and hardly any at S396 or S404 (Fig. 4A). Similarly, T205 (and, less so, S199 and S396) were phosphorylated in p38γ^{CA} transgenic mice (fig. S19). pT205 increased after PTZ in *p38*γ$^{+/+}$ animals but was virtually abolished in *p38*γ$^{-/-}$ mice, whereas pS199, pS396, and pS404 were induced in both *p38*γ$^{+/+}$ and *p38*γ$^{-/-}$ mice (fig. S19). Similarly, pT205 was markedly reduced in APP23.*p38*γ$^{-/-}$ animals compared with APP23.*p38*γ$^{+/+}$ mice (Fig. 4B). In primary neurons, pT205 (but not p199) was markedly reduced by pan-p38 inhibition (fig. S20). Taken together, these findings indicate that pT205 was a primary p38γ site in tau.

Next, we showed that a phosphorylation-mimicking Thr[205]→Glu[205] (T205E) tau variant coprecipitated significantly less with PSD-95 as compared with nonmutant and T205A (A, Ala) tau (Fig. 4C and fig. S21). In contrast, phosphorylation-mimicking mutants of all other identified sites had no effect on PSD-95/tau/Fyn interaction (fig. S18). Microscale thermophoresis and glutathione *S*-transferase–pulldown in vitro and fluorescence-lifetime imaging microscopy (FLIM)–fluorescence resonance energy transfer (FRET) analysis in live cells confirmed the markedly compromised interaction of T205E tau with PSD-95 (fig. S22). The T205E mutation did not hinder tau/Fyn interaction (fig. S21). Phosphorylation of T205 by p38γ^{CA} was required for disrupting PSD-95/tau/Fyn complexes (fig. S21). Hence, p38γ regulated PSD-95/tau/Fyn complexes via phosphorylating tau at T205.

The disruption of NR/PSD-95/tau/Fyn complexes prevents excitotoxicity and Aβ toxicity (*9*). Hence, phosphorylation of tau at T205 should similarly mitigate neurotoxicity. Aβ caused cell death in WT and T205A neurons but significantly less in T205E tau-expressing neurons (fig. S23). Similarly, neurons expressing p38γ and, more so, p38γ^{CA} were significantly more resistant to Aβ-induced cell death than controls (fig. S24). PTZ-induced seizures are reduced in *tau*$^{-/-}$ mice (*8*, *9*). Adeno-associated virus (AAV)–mediated expression of WT and T205A neurons, but not T205E tau or green fluorescent protein (GFP), in the forebrains of *tau*$^{-/-}$ mice enhanced PTZ-induced seizures (Fig. 4D and fig. S25). In contrast, expression of p38γ^{CA} in WT mice using AAV or in Thy1.2-p38γ^{CA} transgenic mice decreased PTZ-induced seizures (fig. S25). AAV-mediated p38γ^{CA} expression in APP23 mice rescued memory deficits and network aberrations; the same was true for crossing APP23 with Thy1.2-p38γ^{CA} mice (Fig. 4, E and F, and figs. S26 and S27). In summary, the levels of active p38γ kinase and tau phosphorylation at T205 determined susceptibility to excitotoxicity and Aβ toxicity.

Here we have shown that T205 phosphorylation of tau is part of an Aβ toxicity–inhibiting response. This is contrary to the current view that tau phosphorylation downstream of Aβ toxicity is a pathological response (*3*). However, this finding is in line with the idea that tau is involved in normal physiologic NR signaling events in neurons (*12*). Finally, we found that tau-dependent Aβ toxicity was modulated by site-specific tau phosphorylation, which inhibited postsynaptic PSD-95/tau/Fyn complexes, revealing an Aβ toxicity–limiting role of p38γ in AD that is distinct and opposite to the effects of p38α and p38β (*11*, *13*, *14*).

REFERENCES AND NOTES

1. C. Ballatore, V. M. Lee, J. Q. Trojanowski, *Nat. Rev. Neurosci.* **8**, 663–672 (2007).
2. C. Haass, D. J. Selkoe, *Nat. Rev. Mol. Cell Biol.* **8**, 101–112 (2007).
3. L. M. Ittner, J. Götz, *Nat. Rev. Neurosci.* **12**, 67–72 (2011).
4. K. Iqbal, F. Liu, C.-X. Gong, A del C. Alonso, I. Grundke-Iqbal, *Acta Neuropathol.* **118**, 53–69 (2009).
5. E. M. Mandelkow, E. Mandelkow, *Cold Spring Harb. Perspect. Med.* **2**, a006247 (2012).
6. E. S. Musiek, D. M. Holtzman, *Nat. Neurosci.* **18**, 800–806 (2015).
7. M. Rapoport, H. N. Dawson, L. I. Binder, M. P. Vitek, A. Ferreira, *Proc. Natl. Acad. Sci. U.S.A.* **99**, 6364–6369 (2002).
8. E. D. Roberson *et al.*, *Science* **316**, 750–754 (2007).
9. L. M. Ittner *et al.*, *Cell* **142**, 387–397 (2010).
10. J. J. Palop, L. Mucke, *Nat. Neurosci.* **13**, 812–818 (2010).
11. G. E. Hardingham, H. Bading, *Nat. Rev. Neurosci.* **11**, 682–696 (2010).
12. L. Mucke, D. J. Selkoe, *Cold Spring Harb. Perspect. Med.* **2**, a006338 (2012).
13. Q. Wang, D. M. Walsh, M. J. Rowan, D. J. Selkoe, R. Anwyl, *J. Neurosci.* **24**, 3370–3378 (2004).
14. S. Li *et al.*, *J. Neurosci.* **31**, 6627–6638 (2011).
15. A. A. Ittner, A. Gladbach, J. Bertz, L. S. Suh, L. M. Ittner, *Acta Neuropathol. Commun.* **2**, 149 (2014).
16. M. A. Fabian *et al.*, *Nat. Biotechnol.* **23**, 329–336 (2005).
17. M. B. Menon, S. Dhamija, A. Kotlyarov, M. Gaestel, *Autophagy* **11**, 1425–1427 (2015).
18. C. Sturchler-Pierrat *et al.*, *Proc. Natl. Acad. Sci. U.S.A.* **94**, 13287–13292 (1997).
19. G. Buzsáki, E. I. Moser, *Nat. Neurosci.* **16**, 130–138 (2013).
20. R. Goutagny, J. Jackson, S. Williams, *Nat. Neurosci.* **12**, 1491–1493 (2009).
21. R. T. Canolty *et al.*, *Science* **313**, 1626–1628 (2006).
22. A. B. Tort, R. W. Komorowski, J. R. Manns, N. J. Kopell, H. Eichenbaum, *Proc. Natl. Acad. Sci. U.S.A.* **106**, 20942–20947 (2009).
23. A. Probst *et al.*, *Acta Neuropathol.* **99**, 469–481 (2000).
24. M. Aarts *et al.*, *Science* **298**, 846–850 (2002).
25. M. Goedert *et al.*, *FEBS Lett.* **409**, 57–62 (1997).

ACKNOWLEDGMENTS

We thank the staff of the Biological Resources Centre of UNSW for animal care, E. Hinde for help with FLIM-FRET experiments, D. Sullivan and T. Foo for *APOE* genotyping of human samples, and T. Saito and T. C. Saido for APP^{NL-G-F} mice. The data from mass spectrometry experiments can be found in the supplementary materials. This work was funded by the National Health and Medical Research Council (grants 1081916, 1037746, and 1003083), the Australian Research Council (grants DP130102027 and DE130101591), Alzheimer's Association (grant NIRG000070035), Alzheimer's Australia (grants DGP14-39 and DGP14-95), the NIH (grant R28AA012725), and UNSW Australia. A.I. and L.M.I. are inventors on Australian patent application number APO/2016/900764, submitted by UNSW, which covers increasing p38γ activity to prevent neuronal toxicity.

SUPPLEMENTARY MATERIALS

www.sciencemag.org/content/354/6314/904/suppl/DC1
Materials and Methods
Figs. S1 to S27
Tables S1 to S5
References (*26*–*53*)

22 July 2016; resubmitted 9 October 2016
Accepted 19 October 2016
10.1126/science.aah6205

Downloaded from http://science.sciencemag.org/ on July 18, 2017

Science

Site-specific phosphorylation of tau inhibits amyloid-β toxicity in Alzheimer's mice

Arne Ittner, Sook Wern Chua, Josefine Bertz, Alexander Volkerling, Julia van der Hoven, Amadeus Gladbach, Magdalena Przybyla, Mian Bi, Annika van Hummel, Claire H. Stevens, Stefania Ippati, Lisa S. Suh, Alexander Macmillan, Greg Sutherland, Jillian J. Kril, Ana P. G. Silva, Joel P. Mackay, Anne Poljak, Fabien Delerue, Yazi D. Ke and Lars M. Ittner

Science **354** (6314), 904-908.
DOI: 10.1126/science.aah6205

Tau phosphorylation—not all bad

Alzheimer's disease presents with amyloid-β (Aβ) plaques and tau tangles. The prevailing idea in the field is that Aβ induces phosphorylation of tau, which in turn mediates neuronal dysfunction. Working in Alzheimer's disease mouse models, Ittner *et al.* found evidence for a protective role of tau in early Alzheimer's disease. This protection involves specific tau phosphorylation at threonine 205 at the postsynapse. A protective role of phosphorylated tau in disease challenges the dogma that tau phosphorylation only mediates toxic processes.

Science, this issue p. 904

ARTICLE TOOLS http://science.sciencemag.org/content/354/6314/904

SUPPLEMENTARY MATERIALS http://science.sciencemag.org/content/suppl/2016/11/16/354.6314.904.DC1

RELATED CONTENT
http://stm.sciencemag.org/content/scitransmed/8/363/363ra150.full
http://stm.sciencemag.org/content/scitransmed/8/340/340ra72.full
http://stm.sciencemag.org/content/scitransmed/8/338/338ra66.full
http://stm.sciencemag.org/content/scitransmed/8/332/332ra44.full
http://stke.sciencemag.org/content/sigtrans/9/426/ec102.abstract
http://stke.sciencemag.org/content/sigtrans/9/421/ec71.abstract
http://stke.sciencemag.org/content/sigtrans/8/384/ra67.full
http://science.sciencemag.org/content/sci/355/6326/eaam9523.full
http://stke.sciencemag.org/content/sigtrans/10/478/eaal2021.full

REFERENCES This article cites 53 articles, 19 of which you can access for free
http://science.sciencemag.org/content/354/6314/904#BIBL

PERMISSIONS http://www.sciencemag.org/help/reprints-and-permissions

Use of this article is subject to the Terms of Service

Science (print ISSN 0036-8075; online ISSN 1095-9203) is published by the American Association for the Advancement of Science, 1200 New York Avenue NW, Washington, DC 20005. 2017 © The Authors, some rights reserved; exclusive licensee American Association for the Advancement of Science. No claim to original U.S. Government Works. The title *Science* is a registered trademark of AAAS.

Downloaded from http://science.sciencemag.org/ on July 18, 2017